A General Bond Graph Approach for Computational Fluid Dynamics
Part II: Applications

[1] Gandolfo Raso, E. F. (egandolfo@uncu.edu.ar), [2] Larreteguy, A. E. (alarreteguy@uade.edu.ar), [3] Baliño, J. L. (balino@cab.cnea.gov.ar)

Centro Atómico Bariloche and Instituto Balseiro, 8400 - S. C. de Bariloche (RN), Argentina

Present addresses:
[1] Universidad Nacional de Cuyo, Ciudad Universitaria, Parque Gral. San Martín, 5500 - Mendoza, Argentina
[2] Universidad Argentina de la Empresa (UADE), Lima 717, 1073 - Buenos Aires, Argentina
[3] Instituto de Pesquisas Energéticas e Nucleares (IPEN), Travessa R, 400 - Cidade Universitaria, São Paulo - SP - CEP 05508-900, Brasil

Abstract

In this paper some examples of application of a general Bond Graph approach for CFD problems, developed in a previous paper by the authors, are shown. One dimensional examples of heat conduction and advection-diffusion problems are presented, and the results are compared to the analytical ones. It can be shown that with very simple (constant) shape functions for entropy, diffusion effects can be modelled rigorously with the aid of generalized (delta) functions. For advection-diffusion problems, upwind schemes can be introduced naturally by means of the weight functions. The treatment of different boundary conditions for these problems in terms of Bond Graph elements is presented. The results obtained with this formalism show excellent agreement with the analytical solutions.

Keywords: Computational Fluid Dynamics, boundary conditions, advection-diffusion problems, upwinding.

1. Introduction

In recent years, it was observed an increasing interest in formulating system models in which fluid dynamic and heat transfer effects are important. In order to solve multidimensional problems with the aid of computer programs, it is important that these models can be implemented numerically. This task, main concern of the area of Computational Fluid Dynamics (CFD), is performed by systematically discretizing the continua, that is, by replacing the continuous variables by a combination of a finite set of nodal values and interpolating functions. The result is a (generally nonlinear) algebraic problem, instead of the original differential or integro-differential one.

The Bond Graph formalism allows a systematic approach for representing and analyzing dynamic systems [1] . Dynamic systems belonging to different fields of knowledge, like Electrodynamics, Solid Mechanics, Fluid Mechanics, etc., can be described in terms of a finite number of variables and basic elements.

An interesting type of problems are those in which heat transport are due to heat conduction and fluid flow. These situations define what are known as advection-diffusion problems [4] . The main characteristic of these problems is that the velocity field and the density are given.

2. Bond Graphs and Heat Transport

The transport of thermal energy due to heat conduction can be written as a product of an absolute temperature θ times an entropy flow $\dot{S}$. The absolute temperature plays the role of generalized effort variable in Bond Graph notation, while the entropy flow plays the role of generalized flow variable.

Entropy generation and irreversibility in heat conduction under finite temperature drop were modelled with the aid of transformers [5] , being the transformer modulus dependent on the operating conditions, or with generalized, power conserving resistance fields [6] [1] [7] . All these representations starts from relatively simple lumped parameter systems and satisfy the conservation of thermal power energy and (with the appropriate definition of parameters) the Second Law of Thermodynamics, this is, entropy production in irreversible processes.

The thermal energy transport associated with the mass flow was not modeled, up to now, in a general fashion. The applications made so far dealt with problem restrictions such as the neglect of inertia terms (which amounts for the major non-linearities) [8] [9] , very simple flow geometries [10] [11] or the use of the so-called "pseudo bond graphs" [12] [13] [14] [15] .

Bond Graph modeling procedures reported in the literature start from lumped-parameter systems, so integration in space and also assumptions related to the resolution scheme are made beforehand.

In [8] the concept of convection bond is presented. A convection bond has one flow (the mass flow) and two efforts (stagnation pressure and stagnation enthalpy). Causal strokes refer to the pair stagnation pressure and mass flow only, leaving the enthalpy determined both physically and computationally for the values defined upstream, this is, assuming a full upwind numerical scheme.

In a recent work [2] [3] a theoretical development of a general Bond Graph approach for CFD was presented. Density, entropy per unit volume and velocity were used as discretized variables; in this way, time-dependent nodal values and interpolation functions were introduced to represent the flow field. Nodal vectors were defined as Bond Graph state variables, namely mass, entropy and velocity. It was shown that the system total energy can be represented as a 3-port IC field. The conservation of linear momentum for the nodal velocity is represented at the inertial port, while mass and entropy conservation equations are represented at the capacitive ports. All kind of boundary conditions are handled consistently and can be represented as generalized modulated effort sources at the inertial port or modulated flow sources at the capacitive ports. In this paper we shall follow this approach, in which the heat conduction and advection terms influence the capacitive port corresponding to the IC field representing the total energy stored in the system.

The motivation of this paper is the application of the theoretical development described above to advection-diffusion problems. Unless stated, the nomenclature used here has to be taken from the companion paper [3] .

3. System Equations

In the following it will be assumed that the velocity field is known and the density is constant, this is:

$$\mathbf{V} = \mathbf{V}(\mathbf{r}, t) \tag{1}$$

3.1 System Bond Graph and State Equations

The resulting system Bond Graph is shown in Fig. 1. At the 0 junction with common $\underline{\Theta}$ we add all the nodal entropy changes per unit time; in this way, the flow balance represents the thermal energy conservation equation for the nodal entropy values. The modulated sources are needed to represent the different boundary conditions established in the problem, as well as to represent volumetric sources. The resulting Bond Graph is a simplification of the one obtained in [3] , in which there is power flow only at the capacitive port and, since the velocity field is known, the terms $\underline{\dot{S}_C}$ and $\underline{\dot{S}_D}$ come from generalized flow sources. From here, the resulting state equations are:

$$\underline{\dot{S}} = -\underline{\dot{S}_C} + \underline{\dot{S}_{QF}} + \underline{\dot{S}_Q^{(\Gamma)}} + \underline{\dot{S}_D} + \underline{\dot{S}_F} \tag{2}$$

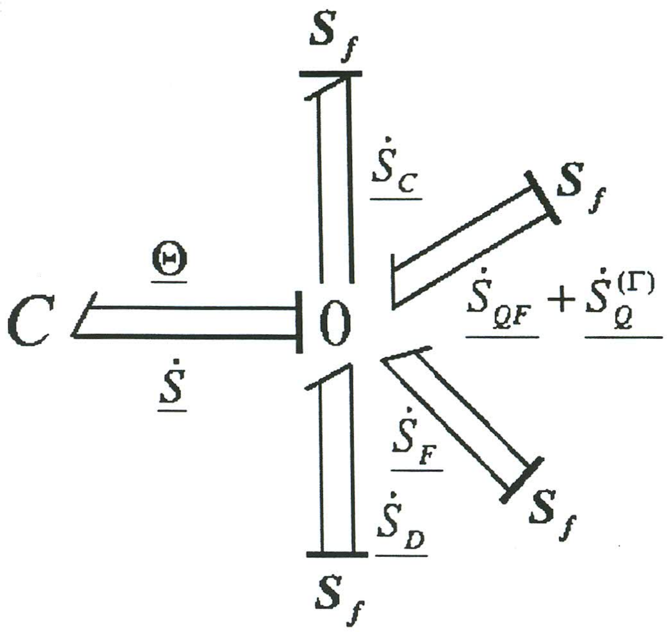

Figure 1: System Bond Graph for advection-diffusion problems.

4. Some exact solutions

In this section we shall obtain and analyze some exact solutions for the entropy per unit volume in advection-diffusion, one-dimensional problems.

4.1 Nondimensional balance equation

The power balance equation for the C field port is [3] :

$$\theta \frac{\partial s_v}{\partial t} = -\theta\, \nabla.(s_v\, \mathbf{V}) - \nabla.\mathbf{q} + \nabla \mathbf{V} : \underline{\underline{\tau}} + \Phi \tag{3}$$

Assuming valid Fourier's law and considering the state equation $\theta = \theta\,(s_v,\, \rho)$ it can be shown that the heat conduction term can be written as:

$$\nabla.\mathbf{q} = -\frac{\lambda\, \theta}{\rho\, c_v} \left[\frac{1}{\rho\, c_v} \,(\nabla s_v)^2 + \nabla^2 s_v \right] \tag{4}$$

From Eq. (4) it can be seen that the power conservation equation is not linear when expressed in terms of the entropy per unit volume. The following nondimensional variables are defined:

$$\mathbf{r}^* = \frac{\mathbf{r}}{L} \tag{5}$$

$$t^* = \frac{U}{L}\, t \tag{6}$$

$$\mathbf{V}^* = \frac{\mathbf{V}}{U} \tag{7}$$

$$s_v^* = \frac{s_v}{\rho\, c_v} \tag{8}$$

$$\underline{\underline{\tau}}^* = \frac{L}{\mu\, U}\, \underline{\underline{\tau}} \tag{9}$$

$$\theta^* = \frac{c_v}{U^2}\, \theta \tag{10}$$

$$\Phi^* = \frac{L}{\rho\, U^3}\, \Phi \tag{11}$$

With these definitions we get, for the non dimensional entropy conservation equation:

$$\begin{aligned} \frac{\partial s_v^*}{\partial t^*} &= -\nabla^*.(s_v^*\, \mathbf{V}^*) + \frac{1}{Pe_L} \left[(\nabla^* s_v^*)^2 + \nabla^{*\,2} s_v^* \right] \\ &\quad + \frac{1}{Re_L}\, \frac{1}{\theta^*}\, \nabla^* \mathbf{V}^* : \underline{\underline{\tau}}^* + \frac{1}{\theta^*}\, \Phi^* \end{aligned} \tag{12}$$

where we define a Peclet number and the Reynolds number correspondingly as:

$$Pe_L = \frac{\rho\, c_v\, U\, L}{\lambda} \tag{13}$$

$$Re_L = \frac{\rho\, U\, L}{\mu} \tag{14}$$

4.2 Some one dimensional solutions

Let us consider a steady, one dimensional problem with constant thermophysical properties. Assuming that the velocity field is uniform ($\mathbf{V} = U\, \mathbf{i}$) and neglecting volumetric heat sources, we have:

$$\left(\frac{\partial s_v^*}{\partial x^*} \right)^2 + \frac{\partial^2 s_v^*}{\partial x^{*\,2}} - Pe_L\, \frac{\partial s_v^*}{\partial x^*} = 0 \tag{15}$$

The solution of Eq. (15) with the boundary conditions:

$$s_v^*\,(x^* = 0) = s_{v0}^* \tag{16}$$

$$s_v^*\,(x^* = 1) = s_{v1}^* \tag{17}$$

is:

$$\begin{aligned} s_v^* - s_{v0}^* &= ln \left[\exp\,(x^*\, Pe_L + \Delta s_v^*) + \exp\,(Pe_L) \right. \\ &\quad \left. - \exp\,(\Delta s_v^*) - \exp\,(x^*\, Pe_L) \right] - (Pe_L - 1) \end{aligned} \tag{18}$$

where:

$$\Delta s_v^* = s_{v1}^* - s_{v0}^* \tag{19}$$

For a pure diffusion problem ($Pe_L = 0$) Eq. (18) reduces to

$$s_v^* - s_{v0}^* = ln \left\{ 1 + x^*\; [\exp\,(\Delta s_v^*) - 1] \right\} \tag{20}$$

Eqs. (18) and (20) look strange because of the nonlinear nature of Eq. (15). Nevertheless, it is easy to recover the solutions in terms of temperature when the thermodynamic state relations are introduced. For a pure substance evolutioning at constant density we have [16] :

$$\theta = \theta_R\, \exp\,(s_v^*) \tag{21}$$

$$\exp\,(\Delta s_v^*) = \exp\,(s_{v1}^* - s_{v0}^*) = \frac{\theta_1}{\theta_0} \tag{22}$$

In Eq. (21) θ_R is a reference temperature for which the entropy is zero. Replacing Eq. (22) correspondingly in Eqs. (18) and (20), we get the well known solutions for the advection-diffusion and heat conduction problems:

$$\frac{\theta - \theta_0}{\theta_1 - \theta_0} = \frac{\exp\,(x^*\, Pe_L) - 1}{\exp\,(Pe_L) - 1} \tag{23}$$

$$\frac{\theta - \theta_0}{\theta_1 - \theta_0} = x^* \tag{24}$$

For small values of the parameter Δs_v^*, Eqs. (18) and (20) reduce correspondingly to:

$$\frac{s_v^* - s_{v0}^*}{s_{v1}^* - s_{v0}^*} \cong \frac{\exp\,(x^*\, Pe_L) - 1}{\exp\,(Pe_L) - 1} \tag{25}$$

$$\frac{s_v^* - s_{v0}^*}{s_{v1}^* - s_{v0}^*} \cong x^* \tag{26}$$

Comparing Eq. (23) with (25) and Eq. (24) with (26), we observe that the approximate entropy solutions coincide with the temperature solutions. The condition $\Delta s_v^* \ll 1$ can be used as a criterion to linearize the balance equation when expressed in terms of the entropy.

5. Examples

In the following, we apply the formalism to the one-dimensional problem corresponding to heat conduction and advection-diffusion in a slab. We assume a uniform velocity field and constant thermophysical properties. Considering n_s entropy nodes, the general system Bond Graph shown in Fig. 1 reduces to the one shown in Fig. 2. It can be observed that the elements of the vector $\underline{\dot{S}_Q^{(\Gamma)}}$, related to the boundary conditions, can be nonzero only for nodes 1 and n_s.

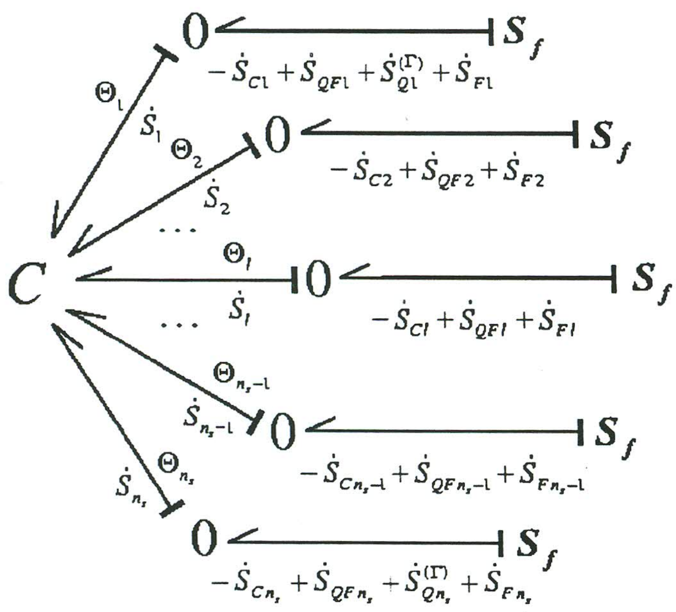

Figure 2: System Bond Graph for one dimensional advection-diffusion problems.

5.1 Heat conduction in a slab

For an inner node ($1 < l < n_s$), we consider the following shape and weight functions:

$$\varphi_{sl} = \begin{cases} 0 & x < -\frac{h}{2} \\ 1 & -\frac{h}{2} < x < \frac{h}{2} \\ 0 & x > \frac{h}{2} \end{cases} \tag{27}$$

$$w_{sl} = \begin{cases} 0 & x < -h \\ 1+\frac{x}{h} & -h < x < 0 \\ 1-\frac{x}{h} & 0 < x < h \\ 0 & x > h \end{cases} \tag{28}$$

In Eq. (27) and (28), x is a local coordinate with origin at the entropy node l, as shown in Fig. 3. It is important to notice that, according to the chosen shape function, the element S_l of the entropy vector is coincident with the entropy corresponding to the control volume located at $-\frac{h}{2} \leq x \leq \frac{h}{2}$. Besides, the shape function is discontinuous at $x = -\frac{h}{2}$ and $x = \frac{h}{2}$. From here we get:

$$\frac{\partial \varphi_{sl}}{\partial x} = \delta\left(x+\tfrac{h}{2}\right) - \delta\left(x-\tfrac{h}{2}\right) \tag{29}$$

$$\frac{\partial w_{sl}}{\partial x} = \begin{cases} 0 & x < -h \\ \frac{1}{h} & -h < x < 0 \\ -\frac{1}{h} & 0 < x < h \\ 0 & x > h \end{cases} \tag{30}$$

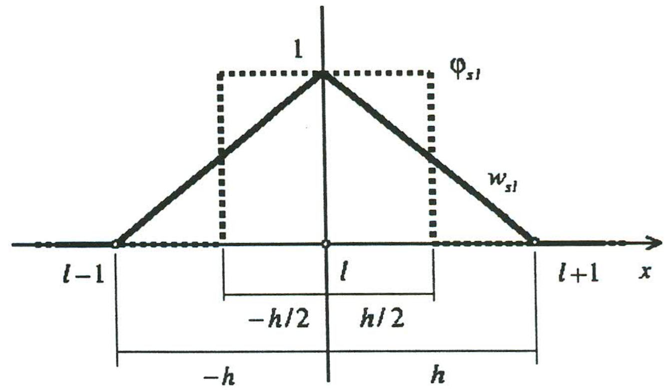

Figure 3: Shape and weight functions for an inner node. The weight function is shown in a continuous line.

$$\frac{\partial s_v}{\partial x} = \sum_{l=1}^{n_s} s_{vl} \frac{\partial \varphi_{sl}}{\partial x} = \left(s_{v\,l} - s_{v\,l-1}\right) \delta\left(x+\tfrac{h}{2}\right)$$
$$+ \left(s_{v\,l+1} - s_{v\,l}\right) \delta\left(x-\tfrac{h}{2}\right) \tag{31}$$

For the first entropy node ($l = 1$) we have:

$$\varphi_{s\,1} = \begin{cases} 1 & 0 < x < \frac{h}{2} \\ 0 & x > \frac{h}{2} \end{cases} \tag{32}$$

$$w_{s\,1} = \begin{cases} 1-\frac{x}{h} & 0 < x < h \\ 0 & x > h \end{cases} \tag{33}$$

$$\frac{\partial \varphi_{s1}}{\partial x} = -\delta\left(x-\tfrac{h}{2}\right) \tag{34}$$

$$\frac{\partial w_{s\,1}}{\partial x} = \begin{cases} -\frac{1}{h} & 0 < x < h \\ 0 & x > h \end{cases} \tag{35}$$

$$\frac{\partial s_v}{\partial x} = \left(s_{v\,2} - s_{v\,1}\right) \delta\left(x-\tfrac{h}{2}\right) \tag{36}$$

For the last entropy node ($l = n_s$) we have:

$$\varphi_{s\,n_s} = \begin{cases} 0 & x < -\frac{h}{2} \\ 1 & -\frac{h}{2} < x < 0 \end{cases} \tag{37}$$

$$w_{s\,n_s} = \begin{cases} 0 & x < -h \\ 1+\frac{x}{h} & -h < x < 0 \end{cases} \tag{38}$$

$$\frac{\partial \varphi_{s\,n_s}}{\partial x} = \delta\left(x+\tfrac{h}{2}\right) \tag{39}$$

$$\frac{\partial w_{s\,n_s}}{\partial x} = \begin{cases} 0 & x < -h \\ \frac{1}{h} & -h < x < 0 \end{cases} \tag{40}$$

$$\frac{\partial s_v}{\partial x} = \left(s_{v\,n_s} - s_{v\,n_s-1}\right) \delta\left(x+\tfrac{h}{2}\right) \tag{41}$$

For these shape and weight functions, we have:

$$\Omega_{sl} = h \qquad (1 < l < n_s) \tag{42}$$

$$\Omega_{s\,1} = \Omega_{s\,n_s} = \frac{h}{2} \tag{43}$$

$$\Theta_l = \theta_l \tag{44}$$

$$S_l = s_{vl}\, \Omega_{sl} \tag{45}$$

$$\underline{\dot{S}_C} = \underline{\dot{S}_D} = \underline{0} \tag{46}$$

$$
\begin{aligned}
\dot{S}_{QFl} &= \frac{1}{\Theta_l}\int_{\Omega} \mathbf{q}\,.\,\nabla w_{sl}\, d\Omega \\
&= -\frac{1}{\theta_l}\int_{-h}^{h} \frac{\lambda\,\theta}{\rho\, c_v}\,\frac{\partial s_v}{\partial x}\,\frac{\partial w_{sl}}{\partial x}\, dx \qquad (47)\\
&= \frac{\lambda}{\rho\, c_v}\,\frac{1}{2\,h}\left[-\frac{\theta_{l-1}}{\theta_l}\,(s_{v\,l}-s_{v\,l-1}) \right.\\
&\quad + (s_{v\,l-1} - 2\,s_{v\,l} + s_{v\,l+1}) \\
&\quad \left. + \frac{\theta_{l+1}}{\theta_l}\,(s_{v\,l+1}-s_{v\,l})\right] \qquad (48)
\end{aligned}
$$

$$
\begin{aligned}
\dot{S}_{QF1} &= -\frac{1}{\theta_1}\int_{0}^{h} \frac{\lambda\,\theta}{\rho\, c_v}\,\frac{\partial s_v}{\partial x}\,\frac{\partial w_{s\,1}}{\partial x}\, dx \\
&= \frac{\lambda}{\rho\, c_v}\,\frac{1}{2\,h}\left[\left(1+\frac{\theta_2}{\theta_1}\right)(s_{v\,2}-s_{v\,1})\right] \qquad (49)
\end{aligned}
$$

$$
\begin{aligned}
\dot{S}_{QFn_s} &= -\frac{1}{\theta_{n_s}}\int_{-h}^{0} \frac{\lambda\,\theta}{\rho\, c_v}\,\frac{\partial s_v}{\partial x}\,\frac{\partial w_{s\,n_s}}{\partial x}\, dx \\
&= -\frac{\lambda}{\rho\, c_v}\,\frac{1}{2\,h}\left[\left(\frac{\theta_{n_s-1}}{\theta_{n_s}}+1\right)(s_{v\,n_s}-s_{v\,n_s-1})\right] \qquad (50)
\end{aligned}
$$

The temperature ratios in Eqs. (48) to (50) can be written in terms of the entropy per unit volume by means of Eq. (22). Finally, the state equations can be obtained by using Eq. (45).

From the analysis made above, it can be seen that the diffusion effects can be modelled rigorously using the simplest shape function (constant) for entropy, with the aid of generalized (delta) functions.

With the shape and weight functions defined above, different problems were solved numerically. We present results for heat conduction in the region $0 \leq x \leq L$, with boundary conditions:

$$\frac{\partial\theta}{\partial x}\,(0,\,t) = 0 \qquad (51)$$

$$-\lambda\,\frac{\partial\theta}{\partial x}\,(L,\,t) = H\,[\theta\,(L,\,t) - \theta_\infty] \qquad (52)$$

and initial condition $\theta(x, 0) = \theta_0$. For this problem, it can be shown [3] that the flow sources needed to establish the boundary conditions at nodes 1 and n_s are, correspondingly:

$$\dot{S}^{(\Gamma)}_{QF\,1} = 0 \qquad (53)$$

$$\dot{S}^{(\Gamma)}_{QF\,n_s} = -H\left(1-\frac{\theta_\infty}{\theta_{n_s}}\right) \qquad (54)$$

The numerical and exact solutions [17] for the nondimensional temperature, shown in Fig. 4, are compared in terms of the following nondimensional parameters:

$$\hat{\theta} = \frac{\theta-\theta_\infty}{\theta_0-\theta_\infty} \qquad (55)$$

$$Bi = \frac{H\,L}{\lambda} \qquad (56)$$

$$Fo = \frac{\alpha_\theta\, t}{L^2} \qquad (57)$$

where Bi and Fo are correspondingly the Biot and Fourier numbers. In Eq. (57) α_θ is a thermal diffusivity, defined as:

$$\alpha_\theta = \frac{\lambda}{\rho\, c_v} \qquad (58)$$

The numerical results shown in Fig. 4 correspond to a fairly large number of nodes (i.e. 201); this has been done on purpose to show that the formulation is indeed spatially consistent. Although good accuracy was also obtained with much coarser grids, this particular problem is very tough for uniform grids, due to the steep temperature profiles that appear for $Fo << 1$.

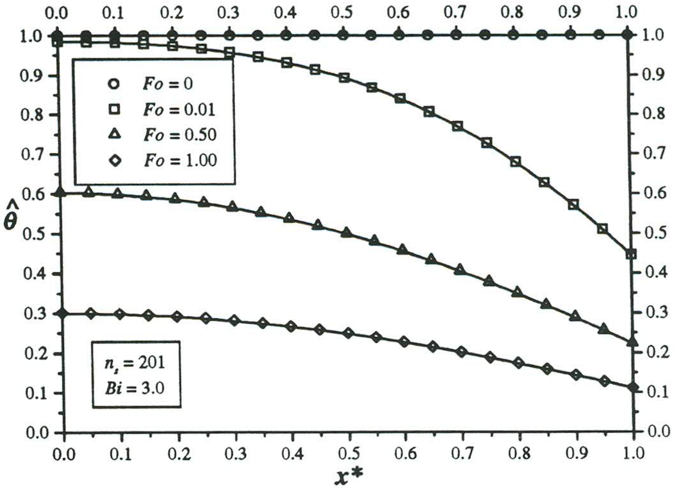

Figure 4: Heat conduction in a slab. Analytical solutions are shown in continuous lines, while calculated values are shown for selected nodes.

5.2 Advection-diffusion in a slab

5.2.1 Linear weight function

For an inner node ($1 < l < n_s$), we have:

$$
\begin{aligned}
\dot{S}_{Cl} &= \frac{1}{\Theta_l}\int_{\Omega} w_{sl}\,\theta\,\nabla.(s_v\,\mathbf{V})\, d\Omega \\
&= \frac{1}{\theta_l}\int_{-h}^{h} w_{sl}\,\theta\, U\,\frac{\partial s_v}{\partial x}\, dx \qquad (59)\\
&= \frac{1}{4}\,U\left[\frac{\theta_{l-1}}{\theta_l}\,(s_{v\,l}-s_{v\,l-1}) \right.\\
&\quad + (s_{v\,l+1} - s_{v\,l-1}) \\
&\quad \left. + \frac{\theta_{l+1}}{\theta_l}\,(s_{v\,l+1}-s_{v\,l})\right] \qquad (60)
\end{aligned}
$$

For the first and last entropy node correspondingly we have:

$$
\begin{aligned}
\dot{S}_{C\,1} &= \frac{1}{\theta_1}\int_{0}^{h} w_{s\,1}\,\theta\, U\,\frac{\partial s_v}{\partial x}\, dx \\
&= \frac{1}{4}\,U\left(1+\frac{\theta_2}{\theta_1}\right)(s_{v\,2}-s_{v\,1}) \qquad (61)
\end{aligned}
$$

$$
\begin{aligned}
\dot{S}_{C\,n_s} &= \frac{1}{\theta_{n_s}}\int_{-h}^{0} w_{s\,n_s}\,\theta\, U\,\frac{\partial s_v}{\partial x}\, dx \\
&= \frac{1}{4}\,U\left(\frac{\theta_{n_s-1}}{\theta_{n_s}}+1\right)(s_{v\,n_s}-s_{v\,n_s-1}) \qquad (62)
\end{aligned}
$$

We present results for the advection-diffusion problem in the region $0 \leq x \leq L$, with boundary conditions:

$$\theta\,(0,\,t) = \theta_0 \qquad (63)$$

$$\theta\,(L,\,t) = \theta_L \qquad (64)$$

and initial condition $\theta(x, 0) = \theta_0$. For this problem, it can be shown [3] that the flow sources needed to establish the boundary conditions at nodes 1 and n_s are, correspondingly:

$$\dot{S}^{(\Gamma)}_{QF\ 1} = \dot{S}_{C\ 1} - \dot{S}_{QF\ 1} \tag{65}$$

$$\dot{S}^{(\Gamma)}_{QF\ n_s} = \dot{S}_{C\ n_s} - \dot{S}_{QF\ n_s} \tag{66}$$

The numerical and exact solutions for steady state are shown in Fig. 5, where the nondimensional temperature is defined as:

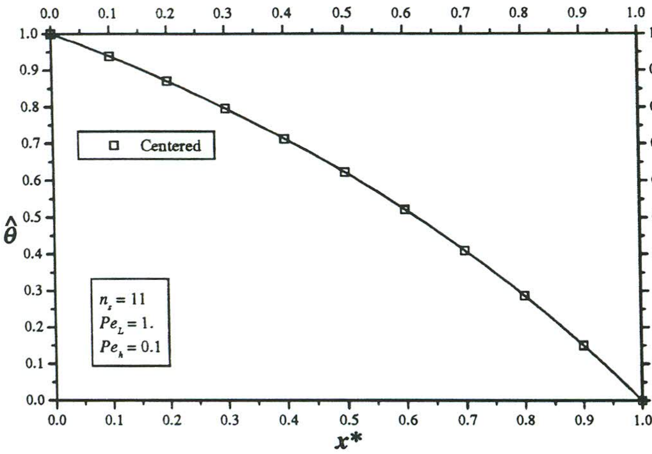

Figure 5: Advection-diffusion in a slab, steady state. Linear weight function, no upwind. The analytical solution is shown in a continuous line.

$$\hat{\theta} = \frac{\theta - \theta_L}{\theta_0 - \theta_L} \tag{67}$$

The solutions obtained show a known behavior: for grid Peclet numbers greater than a critical value ($Pe_{hc} = 2$), the numerical results present oscilations and are no longer a good approximation of the analytical solution (see Fig. 7).

5.2.2 An upwind scheme

A remedy for these unrealistic oscilations in the solution obtained with the linear weight function in advection-diffusion problems is the introduction of upwind schemes. Upwind schemes basically weight unevenly the advected properties corresponding to the points located upstream, compared to the points located downstream. We have found that, in the Bond Graph formalism, the introduction of upwind schemes can be performed naturally through the weight functions.

As an example of an upwind scheme [18] , we propose the following weight function at an inner node ($1 < l < n_s$) (see Fig. 6):

$$w_{sl} = \begin{cases} 0 & x < -h \\ 1 + \frac{x}{h} + \beta & -h < x < 0 \\ 1 - \frac{x}{h} - \beta & 0 < x < h \\ 0 & x > h \end{cases} \tag{68}$$

$$\frac{\partial w_{sl}}{\partial x} = \begin{cases} 0 & x < -h \\ \beta\,\delta(x+h) & x = -h \\ \frac{1}{h} & -h < x < 0 \\ -2\,\beta\,\delta(x) & x = 0 \\ -\frac{1}{h} & 0 < x < h \\ \beta\,\delta(x-h) & x = h \\ 0 & x > h \end{cases} \tag{69}$$

where β is a parameter independent of position, which must be optimized in order to satisfy a specified condition, regarding the accuracy of the solution given by the numerical scheme compared to the exact solution.

For the first and last entropy node we have:

$$w_{s\ 1} = \begin{cases} 1 - \frac{x}{h} - \beta & 0 < x < h \\ 0 & x > h \end{cases} \tag{70}$$

$$\frac{\partial w_{s\ 1}}{\partial x} = \begin{cases} -\frac{1}{h} & 0 < x < h \\ \beta\,\delta(x-h) & x = h \\ 0 & x > h \end{cases} \tag{71}$$

$$w_{s\ n_s} = \begin{cases} 0 & x < -h \\ 1 + \frac{x}{h} + \beta & -h < x < 0 \end{cases} \tag{72}$$

$$\frac{\partial w_{s\ n_s}}{\partial x} = \begin{cases} 0 & x < -h \\ \beta\,\delta(x+h) & x = -h \\ \frac{1}{h} & -h < x < 0 \end{cases} \tag{73}$$

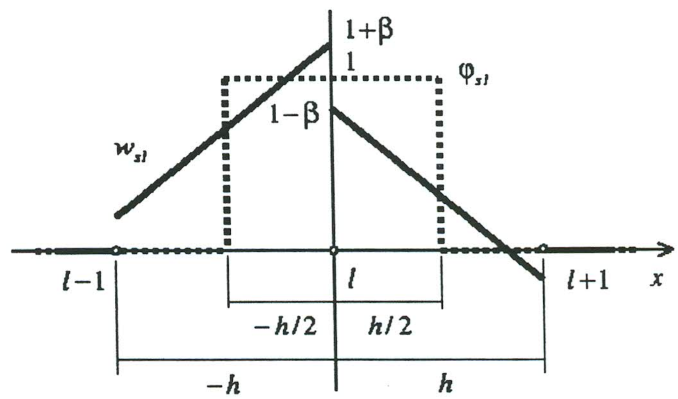

Figure 6: Shape and weight functions with upwind for an inner node. The weight function is shown in a continuous line.

One of the advantages of this upwind scheme is that the conduction term remains unchanged, so Eqs. (48), (49) and (50) are still valid. The entropy advection term results:

$$\begin{aligned} \dot{S}_{Cl} \;=\; & \tfrac{1}{2}\,U\,\Big\{ \frac{\theta_{l-1}}{\theta_l}\,\left(\tfrac{1}{2}+\beta\right)\,(s_{v\ l} - s_{v\ l-1}) \\ & + \left(\tfrac{1}{2}+\beta\right)\,(s_{v\ l} - s_{v\ l-1}) \\ & + \left(\tfrac{1}{2}-\beta\right)\,(s_{v\ l+1} - s_{v\ l}) \\ & + \frac{\theta_{l+1}}{\theta_l}\,\left(\tfrac{1}{2}-\beta\right)\,(s_{v\ l+1} - s_{v\ l}) \Big\} \end{aligned} \tag{74}$$

$$\dot{S}_{C\ 1} = \tfrac{1}{2}\,U\,\left(\tfrac{1}{2}-\beta\right)\left(1 + \frac{\theta_2}{\theta_1}\right)\,(s_{v\ 2} - s_{v\ 1}) \tag{75}$$

$$\dot{S}_{C\ n_s} = \tfrac{1}{2}\,U\,\left(\tfrac{1}{2}+\beta\right)\left(\frac{\theta_{n_s-1}}{\theta_{n_s}} + 1\right)\,(s_{v\ n_s} - s_{v\ n_s-1}) \tag{76}$$

The calculation of the optimal value of β is performed by setting the condition that the numerical scheme has to give the exact steady state value for the entropy at the node l for given values of the entropy at the nodes $l-1$ and $l+1$. Therefore, regarding Eq. (18) we have:

$$s^*_{v\ l-1} \equiv s^*_v\,(x^* = 0) \tag{77}$$

$$s^*_{v\ l} \equiv s^*_v\,(x^* = \tfrac{1}{2}) \tag{78}$$

$$s^*_{v\ l+1} \equiv s^*_v\,(x^* = 1) \tag{79}$$

We define the following quantities:

$$\Delta s^{*\,-}_v = s^*_{v\ l} - s^*_{v\ l-1} \tag{80}$$

$$\Delta s^{*\,+}_v = s^*_{v\ l+1} - s^*_{v\ l} \tag{81}$$

Taking into account Eq. (18) and Eqs. (77) to (81), and since the characteristic length L in Eq. (18) corresponds to $2\,h$ we have:

$$\begin{aligned} \Delta s_v^{*\,-} &= ln\left[\exp\left(Pe_h + \Delta s_v^{*\,-} + \Delta s_v^{*\,+}\right)\right. \\ &\quad + \exp\left(2\,Pe_h\right) - \exp\left(\Delta s_v^{*\,-} + \Delta s_v^{*\,+}\right) \\ &\quad \left. - \exp\left(Pe_h\right)\right] - \left(2\,Pe_h - 1\right) \end{aligned} \tag{82}$$

$$\begin{aligned} \Delta s_v^{*\,+} &= ln\left[\exp\left(2\,Pe_h + \Delta s_v^{*\,-} + \Delta s_v^{*\,+}\right)\right. \\ &\quad \left. - \exp\left(\Delta s_v^{*\,-} + \Delta s_v^{*\,+}\right)\right] \\ &\quad - ln\left[\exp\left(Pe_h + \Delta s_v^{*\,-} + \Delta s_v^{*\,+}\right)\right. \\ &\quad + \exp\left(2\,Pe_h\right) - \exp\left(\Delta s_v^{*\,-} + \Delta s_v^{*\,+}\right) \\ &\quad \left. - \exp\left(Pe_h\right)\right] \end{aligned} \tag{83}$$

where $Pe_h = \dfrac{\rho\, c_v\, U\, h}{\lambda}$ is the Peclet number based on the grid spacing. Taking into account Eq.(22), the state equation corresponding to node l considering steady state can be written as:

$$\begin{aligned} 0 &= -\Delta s_v^{*\,-}\ \exp\left(-\Delta s_v^{*\,-}\right) + \left(\Delta s_v^{*\,+} - \Delta s_v^{*\,-}\right) \\ &\quad + \Delta s_v^{*\,+}\ \exp\left(\Delta s_v^{*\,+}\right) \\ &\quad - Pe_h\ \left[\left(\tfrac{1}{2} + \beta\right)\ \Delta s_v^{*\,-}\ \exp\left(-\Delta s_v^{*\,-}\right)\right. \\ &\quad + \left(\tfrac{1}{2} + \beta\right)\ \Delta s_v^{*\,-} + \left(\frac{1}{2} - \beta\right)\ \Delta s_v^{*\,+} \\ &\quad \left. + \left(\tfrac{1}{2} - \beta\right)\ \Delta s_v^{*\,+}\ \exp\left(\Delta s_v^{*\,+}\right)\right] \end{aligned} \tag{84}$$

Elimination of $\Delta s_v^{*\,-}$ and $\Delta s_v^{*\,+}$ can't be performed analytically from Eqs. (82) and (83). Nevertheless, for $\Delta s_v^{*\,-} \ll 1$ and $\Delta s_v^{*\,+} \ll 1$ it can be shown that:

$$\frac{\Delta s_v^{*\,+}}{\Delta s_v^{*\,-}} \cong \exp(Pe_h) \tag{85}$$

$$\beta \cong -\frac{1}{Pe_h} + \frac{1}{2}\,\frac{\exp(Pe_h) + 1}{\exp(Pe_h) - 1} \tag{86}$$

It can be verified that β is an antisymmetric function, with the asymptotic values $\pm\,\frac{1}{2}$ for $Pe_h \to \pm\,\infty$. For $\beta = \frac{1}{2}$, the properties located downstream have no influence in the integration, and viceversa. With the optimal value of β it was observed that the solutions obtained are all consistent, even for very high Peclet numbers, as shown in Fig. 7.

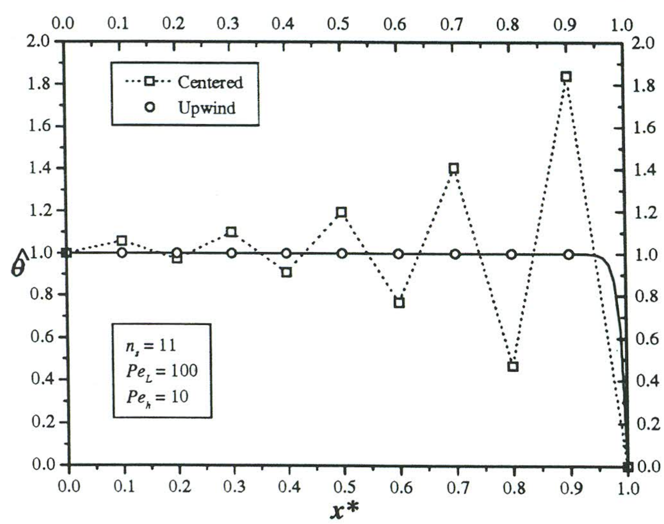

Figure 7: Advection-diffusion in a slab, steady state. Linear weight function, upwind. The analytical solution is shown in a continuous line.

6. Conclusions

The methodology based on Bond Graphs developed by the authors in a companion paper was succesfully applied to one dimensional diffusion (heat conduction) and advection-diffusion problems. It can be shown that with very simple (constant) shape functions for entropy, diffusion effects can be modelled rigorously with the aid of generalized (delta) functions. For advection-diffusion problems, upwind schemes can be introduced naturally by means of the weight functions. The numerical results obtained show excellent agreement with the analytical solutions. Although only one-dimensional cases were presented here, the proposed methodology is completely general, and can be applied as well to multidimensional problems. We authors certainly believe that this work and the companion theoretical paper is the foundation of a bridge between Bond-Graphs and Computational Fluid Dynamics, two fields that have been following almost separate paths until now.

Acknowledgments

E. F. Gandolfo wish to thank FOMEC (Fondo para el Mejoramiento de la Calidad Universitaria) for the financial support obtained to accomplish this work.

References

[1] Karnopp D.C., Margolis D.L. & Rosenberg R.C., System Dynamics: a Unified Approach, 2nd Ed., Wiley Interscience, ISBN 0-471-62171-4, 1990.

[2] Baliño, J. L., Larreteguy, A. E. & Gandolfo, E. F., A General Bond Graph Approach for Computational Fluid Dynamics, submitted to *J. Franklin Inst.*, February 2000.

[3] Baliño, J. L., Larreteguy, A. E. & Gandolfo, E. F., A General Bond Graph Approach for Computational Fluid Dynamics. Part I: Theory, somewhere in this Proceeding.

[4] Patankar, S. V., Numerical Heat Transfer and Fluid Flow, Hemisphere Publishing Corporation, ISBN 0-07-048740-5, 1980.

[5] Thoma, J. U., Bond Graphs for Thermal Energy Transport and Entropy Flow, *J. Franklin Inst.*, Vol. 292, Number 2, 1971.

[6] Thoma, J. U., Entropy and Mass Flow for Energy Conversion, *J. Franklin Inst.*, Vol. 299, Number 2, 1975.

[7] Cellier, F.E., *Continuous System Modeling*, Springer-Verlag, ISBN 0-387-97502-0, 1991.

[8] Brown, F. T., Convection Bonds and Bond Graphs, *J. Franklin Inst.*, Vol. 328, Number 5/6, pp. 871-886, 1991.

[9] Brown, F. T., Applications of Convection Bonds, *ICBGM'99*, The Society for Computer Simulation, pp. 24-29. ISBN 1-56555-155-9, 1999.

[10] Beaman, J. J. & Breedveld, P.C., Physical Modeling with Eulerian Frames and Bond Graphs, *Journal of Dynamic Systems, Measurement and Control*, Vol. 110, pp. 182-188.

[11] Strand, K. & Engja, H., Bond Graph interpretation of One-Dimensional Fluid Flow, *J. Franklin Inst.*, Vol. 328, Number 5/6, pp. 781-793, 1991.

[12] Karnopp, D.C., State variables and Pseudo Bond Graphs for Compressible Thermofluid Systems, *ASME Journal of Dynamic Systems, Measurement and Control*, Vol. 101, No. 3, pp. 201-204.

[13] Tylee, J. L., Pseudo Bond Graph Representation of PWR Pressurizer Dynamics, *Journal of Dynamic Systems, Measurement and Control*, Vol. 105, pp. 255-261, 1983.

[14] Moksnes, P. O. & Engja, H., Application of Bond Graphs to Thermo-Fluid Two-Phase Systems, *ICBGM'99*, The Society for Computer Simulation, pp. 183-188. ISBN 1-56555-155-9, 1999.

[15] Pedersen, E., Modelling Thermodynamic Systems with Changing Gas Mixtures, *ICBGM'99*, The Society for Computer Simulation, pp. 189-195. ISBN 1-56555-155-9,1999.

[16] Callen, H. B., *Thermodynamics*, John Wiley & Sons, Inc., 1960.

[17] Carslaw, H. S.& Jaeger, J. C., Heat Conduction in Solids, Second Edition, Oxford University Press, 1959.

[18] Hughes, T. J. R., A simple scheme for developing "upwind " finite elements, *Int. Journal for Numerical Methods in Engineering*, Vol. 12, pp. 1359-1365, 1978.